

Determining the mass of the accreting white dwarf in magnetic CVs using *RXTE* data

Gavin Ramsay

Mullard Space Science Laboratory, University College London, Holmbury St. Mary, Dorking, Surrey, RH5 6NT

Accepted 20 Dec 1999:

ABSTRACT

We have extracted spectra of 20 magnetic Cataclysmic Variables (mCVs) from the *RXTE* archive and fitted them using the X-ray continuum method of Cropper et al to determine the mass of the accreting white dwarf in each system. We find evidence that the mass distribution of these mCVs is significantly different to that of non-magnetic isolated white dwarfs, with the white dwarfs in mCVs being biased towards higher masses. It is unclear if this effect is due to a selection effect or whether this reflects an real difference in the parent populations.

Key words: accretion – methods: data analysis – cataclysmic variables – stars: fundamental parameters – white dwarfs – X-rays: stars

1 INTRODUCTION

The mass of the accreting white dwarf in a magnetic cataclysmic variable (mCV) is a fundamental property of these binary systems. It is one of the main parameters characterizing the emission from the accretion region. This is because the temperature at the shock front ($T > 10^8$ K) is determined by the mass of the white dwarf, M_{wd} . The post-shock region (the region between the shock front and the surface of the white dwarf) cools mainly by bremsstrahlung radiation. If the magnetic field is sufficiently strong, ($B \gtrsim 10$ MG), then a significant amount of energy can also be radiated away as cyclotron radiation.

Recently several groups have made estimates of M_{wd} in a number of mCVs using X-ray data. These groups have used one of two techniques to derive M_{wd} : the continuum method, where the slope of the X-ray continuum is fitted, and the X-ray line method where the intensity ratio of different emission line species is used. Both of these methods have their difficulties. In the case of the line method (Fujimoto & Ishida 1997, Ezuka & Ishida 1999), this method is more suited in determining M_{wd} for low mass systems. This is because in high mass systems the lines that are used are formed close to the surface of the white dwarf and therefore do not accurately reflect the shock temperature (Cropper, Wu & Ramsay 1999). For low mass systems this is less of a problem. In the case of the continuum method (Cropper, Ramsay & Wu 1998 and Cropper et al 1999), absorption effects can be complex and lead to poor fits to the data. For low mass systems, these methods agree remarkably well: in the case of EX Hya the best fit masses agree to within $0.02 M_{\odot}$.

In this paper, the continuum method is used to determine M_{wd} in 20 mCVs. In a series of papers (Cropper, Ramsay & Wu 1998 and Cropper et al 1999), we have added refinements to our model of the post-shock region. These improvements include adding the effects of cyclotron radiation as a source of cooling, allowing for the fact that the post-shock region is multi-temperature rather than single temperature, and adding a gravitational potential over the height of the post-shock region. While these improvements to our model do not necessarily improve the statistical quality of the fits to the X-ray data, they are essential if accurate masses are to be derived.

As well as modelling the emission spectrum of the post shock region accurately, the absorption, both internal and external to the binary system, has to be taken into account. Cropper et al (1999) showed that the model chosen to account for this absorption can effect the resulting value of M_{wd} to a small degree. For instance, they found some evidence that a partial covering model gave lower masses than an ionised absorber. In reality, the absorption model will be much more complex than either of these models.

A more surprising result from Ramsay et al (1998) was that the mass of the eclipsing mCV XY Ari using *Ginga*, *RXTE* and *ASCA* data was significantly different in the different detectors. However, they found the mass determined using *RXTE* data was consistent with that determined from eclipse studies. Since *RXTE* has a much higher energy response than *Ginga* and *ASCA* it samples an energy range which is closer to the shock temperature. Because of this we expect that the masses derived using *RXTE* data will be more accurate than that of Cropper et al (1999). Therefore to increase our sample of accurate M_{wd} in mCVs, we

have extracted data from the *RXTE* archive. The resulting mass distribution will be compared with that of non-magnetic white dwarfs.

2 THE OBSERVATIONS

RXTE was launched in 1995 Dec, its prime aim being to observe sources with maximum time resolution and moderate energy resolution ($\sim 1\text{keV}$ at 6keV). From the *RXTE* data archive we have extracted data from 6 strong field mCVs (those systems where the magnetic field is sufficiently strong – $B \sim 10\text{--}200\text{MG}$ – to synchronize the spin period of the white dwarf with the binary orbit – the polars) and 13 low field mCVs (those systems where the magnetic field is not sufficiently strong – $B \sim 1\text{--}10\text{MG}$ – to synchronise the spin and orbital periods – the intermediate polars, or IPs). It is not the intention to perform a complete analysis of the data on each system: indeed, for several systems this has already been done elsewhere. Rather, the objective is to extract suitable data from each source and determine M_{wd} .

Data were extracted only if the full set of data was present in the archive (rather than only satellite slewing data which is added to the archive much earlier than the full set of data). Data were cleaned using standard *FTOOLS* procedures. To improve the signal-to-noise ratio, we extracted data using only the top Xenon layer of each PCA. Since *RXTE* is not an imaging X-ray telescope, background subtraction is a particularly important issue. The background is not well characterised before 1996 April 15, so we did not extract data taken before this date. The background was estimated using *PCBACKEST* v2.1b and we used the faint source models applicable to the date of the observation.

Table 1 lists the sources for which data were extracted. It also shows the date of the observations, the exposure of the spectrum used in the analysis and the mean count rate (2–20keV) per PCU of this spectrum. The total exposure of the observations was in most cases greater than the exposure shown in Table 1. In many mCVs an X-ray spectral variation is observed over the course of the spin period of the white dwarf and/or the binary orbital period in the case of the IPs. In these systems, using an integrated spectrum may result in either a poor fit to the data or may effect the resulting determination of M_{wd} . Therefore, in the majority of systems a spectrum was extracted which covered particular spin and/or orbital phases: this is tabulated in the last column of Table 1. In addition, two of the polars in our sample are slightly asynchronous: BY Cam and V1432 Aql. In order that a spectral variation due to the spin-orbit beat interval was not present in the resulting spectrum, we selected data covering a much shorter time interval than the beat period (BY Cam: $P_{beat}=14.5$ days, V1432 Aql: $P_{beat}=49.5$ days).

3 THE MODEL

In modelling the emission spectrum we use the multi-temperature model of Cropper, Ramsay & Wu (1998) with the modifications of Cropper et al (1999) which includes the effects of varying the gravitational potential within the height of the shock region. We take the mean molecular mass of the plasma to be cosmic ($\mu=0.615$). The ratio of cyclotron

to bremsstrahlung cooling, ϵ_o , was fixed for each system. In case of the IPs, this was fixed at the low value of 0.001. By inverting equation 10 of Wu et al (1994) we find we have imposed a magnetic field strength of $B=1\text{--}5$ MG in these systems (depending on the spectrum). For the polars, we fixed ϵ_o at a value which gave field strengths consistent with the known field strength for each system.

For the absorption column, we use two basic models: one or more partial covering models of cold material and the other a partially ionised absorber of the type described by Cropper, Ramsay & Wu (1998). A cold absorber was also present in addition to both these models to account for interstellar absorption. As noted above, both of these models are expected to be simplifications of what is likely to be present in mCVs.

4 THE FITS

A spectrum was extracted from each source covering the energy range 2–20keV and binned so there was a minimum of 50 counts in each spectral element. We found that it was difficult to model the energy range between 6.2–7.2keV in many systems. This is probably due to reflection and fluorescence effects in this energy range which are difficult to accurately model and also because there is an absorption edge at 7.1keV which becomes prominent at high absorbing columns. Because the Pulse Channel Analyser (PCA) has a limited energy resolution ($\sim 1\text{keV}$ at 6keV), it is to be expected that excluding some energy channels will effect the fit to some degree. To test this, we used one of the highest signal to noise spectra (FO Aqr) and excluded data in the energy range 6.0–7.5keV. This had no effect ($<0.01M_\odot$) on the resulting best fit to M_{wd} although the fit was significantly improved. We therefore excluded this energy range in our fits.

We show in Tables 2 and 3 the best fit values of M_{wd} together with the goodness of fit for our sample of polars and IPs. In the case of the polars we also show the fits obtained with a single cold absorber. For the IPs a single cold absorber was not sufficient to fit the data (with the exception of RX 1238–38) so these fits are not shown in Table 3. For two IPs, EX Hya and RX J1712–24, and 2 polars, BY Cam and CP Tuc, good fits were not obtained (the results of these poor fits are not shown in Tables 2 and 3).

There are several possible causes for these poor fits. One is poor background subtraction. There is no evidence that there are problems with background subtraction at the dates of these observations (*RXTE* helpdesk). Since the cosmic ray component of the background model is dependent on galactic latitude, and the background model assumes a high galactic latitude for the object in question, it is possible that this could introduce an error, since the IPs with poor fits have low galactic latitude (EX Hya: $b = +33^\circ$, RX J1712–24: $b = +8^\circ$). However, other sources in our sample which have similar, or even lower galactic latitude, have good fits. We can use the fact that two sources in our sample are eclipsing systems (V2301 Oph and XY Ari) to test how well the background has been subtracted. In both systems, the mean count rate during the eclipse is consistent with zero. Whilst we cannot completely exclude the possibility that the poor fits are due to poor background subtraction, it is more

Source	Date	Exp (sec)	Ct/s/PCU	Phase
V1432 Aql	Jul 1996	4176	3.3	Spin max
BY Cam	June 1997	39712	3.5	Orbital max
V834 Cen	Aug 1997	17872	1.6	Integrated
AM Her	Aug 1998	4048	16.7	Spin max
BL Hyi	Sept 1997	1584	3.9	Primary pole
V2301 Oph	May 1997	5248	3.7	Spin max
CP Tuc	July 1997	28496	2.8	Spin max
FO Aqr	May 1997	25296	6.7	Spin max
XY Ari	Jul – Aug 1996	32384	1.1	Integrated but excluding flare
V405 Aur	Apr 1996	25568	2.8	Integrated
V709 Cas	Mar 1997	13328	6.0	Spin min
BG CMi	Jan 1997	44016	2.7	Integrated
TV Col	Aug 1996	17440	6.6	Orbital max
TX Col	Mar 1997	27600	2.4	Spin max
EX Hya	Jun 1996	18144	9.6	Spin min (exclude orb min)
AO Psc	Sep 1997	13888	6.6	Spin max (exclude orb min)
V1223 Sgr	Nov 1997	6368	12.3	Spin max
V1062 Tau	Feb 1998	22944	3.8	Spin max
RX J1238–38	Jan 1997	29456	1.6	Spin max
RX J1712–24	May 1996	7792	13.8	Orbital max

Table 1. The log of *RXTE* observations of polars (top) and intermediate polars (bottom) used in this paper. In columns 2 & 3 we show the date of the observation and the exposure of the spectrum used in the analysis. In the 4th column we show the mean count rate (2–20keV) per PCU. In the 5th column we show which part of the spin/orbital cycle has been used to make the spectrum used in the analysis.

likely that the residuals are due to the effects of complex absorption.

To test if it is possible to obtain good fits to the data by excluding a larger energy range, we again examined the spectrum of FO Aqr in more detail. Initially we excluded data below 8keV from the fitting process. In comparison with the best fit mass obtained when we included all the spectral channels except 6.0–7.5keV, we found the best fit mass was within $0.05 M_{\odot}$ of this best fit. However, the fit was not very well constrained. By including the energy range covering 5–6keV (where there are no absorption edges) we found that the best fit was within $0.05 M_{\odot}$ and constrained to within $0.1 M_{\odot}$ (at the 90 percent confidence interval). This gave us some confidence that reasonably accurate masses could be obtained for EX Hya, RX J1712–24, CP Tuc and BY Cam even when certain energy ranges are excluded. In the case of EX Hya, RX J1712–24 and BY Cam, energies below 5keV and between 6.0–7.5keV were excluded. In the case of CP Tuc, energies between 6.0–8.5keV were excluded. The masses and goodness of fits to the data shown in Table 2 & 3 for these 4 systems were obtained by these means.

In the case of our polar sample, all systems, with the exception of V1432 Aql, were well fitted with a simple cold absorber (the addition of a more complex absorber did not improve the fit). This is not altogether surprising since no disk is present in these systems. V1432 Aql is a near synchronous system, as is BY Cam where we had to ignore data below 5keV to get a good fit. Observations of another near synchronous system RX J2115–58 (Ramsay et al 1999) suggest that the accretion flow in these systems is complex and at certain beat phases, the stream does not attach itself onto the most favourable magnetic field lines. This may increase

the amount of absorption present in the system and make it hard to model accurately.

In our sample of IPs, the fits using the cold absorber plus partial covering model (CA+PC) was very similar to, or better than the model using a cold absorber plus ionised absorber (CA+IA). In two systems (FO Aqr and V709 Cas) good fits could not be achieved using the CA+IA model. The mean mass for IPs with a CA+PC absorber model was lower ($M_{wd} = 0.85 \pm 0.21$) compared with the CA+IA absorber model ($M_{wd} = 0.96 \pm 0.34$). This is similar to that found by Cropper et al (1999).

In the case of the eclipsing systems (the polar V2301 Oph and the IP XY Ari) we can compare our results with that of mass estimates obtained from eclipse studies. In the case of V2301 Oph we that find our mass of $0.75 \pm 0.05 M_{\odot}$ is consistent with that of $0.80 \pm 0.06 M_{\odot}$ (Silber et al 1994) and $0.9 \pm 0.1 M_{\odot}$ (Barwig, Ritter & Bärnbantner 1994). In the case of XY Ari, Ramsay et al (1998) found a mass of $0.78–1.03 M_{\odot}$. This compares with $0.80–1.13 M_{\odot}$ using a CA+PC absorber model and $>1.25 M_{\odot}$ using CA+IA absorber model. (We note that the masses quoted in Table 3 for XY Ari differ from that quoted in Cropper et al (1999) since the background model applied here is more accurate than that applied previously). This together with the generally better fits obtained using the CA+PC model for our IP sample suggests that this model is a better approximation of the absorption present in mCVs compared with the CA+IA model. We therefore use the masses obtained using this model for the remainder of the paper.

5 DISCUSSION

Source	CA	CA + PC		CA + IA
	$M_{\odot}(\chi^2_{\nu}, \text{dof}, \text{range})$	$M_{\odot}(\chi^2_{\nu}, \text{dof}, \text{range})$	$M_{\odot}(\chi^2_{\nu}, \text{dof}, \text{range})$	
V1432 Aql	1.34 (1.05, 47dof: >1.30)	0.98 (0.56, 45dof: 0.78–1.19)	1.27 (0.95, 45dof: >1.23)	
BY Cam	1.04 (1.04, 32dof: 0.95–1.16)	1.04 (1.11, 30dof: 0.95–1.16)	1.04 (1.12, 30dof: 0.95–1.16)	
V834 Cen	0.68 (0.74, 40dof: 0.63–0.72)	0.66 (0.77, 38dof: 0.61–0.71)	0.64 (0.71, 38dof: 0.62–0.71)	
AM Her	0.73 (0.98, 40dof: 0.70–0.76)	0.74 (1.14, 38dof: 0.71–0.77)	0.73 (1.03, 38dof: 0.70–0.76)	
BL Hyi	0.71 (0.55, 39dof: 0.63–0.78)	0.71 (0.58, 37dof: 0.67–0.79)	0.71 (0.59, 37dof: 0.67–0.79)	
V2301 Oph	0.75 (0.95, 38dof: 0.70–0.80)	0.74 (1.00, 36dof: 0.70–0.80)	0.75 (0.99, 36dof: 0.70–0.80)	
CP Tuc	0.68 (1.37, 34dof: 0.65–0.70)	0.73 (1.51, 32dof: 0.70–0.78)	0.73 (1.51, 32dof: 0.70–0.78)	

Table 2. The results for the fits to our polar data. The fits using three different models are shown. The emission model was the same in all cases and is that described in Cropper et al (1999). In the first model, the absorption is a cold absorber (CA), the next a CA plus partial covering model (PC) and the third a CA plus ionised absorber (IA). The energy range 6.0–7.5keV was excluded in the fits with the exception of BY Cam and CP Tuc where an additional energy range was excluded (see text). The confidence interval for M_{wd} is the 90 per cent interval.

Source	CA + PC	CA + IA
	$M_{\odot}(\chi^2_{\nu}, \text{dof}, \text{range})$	$M_{\odot}(\chi^2_{\nu}, \text{dof}, \text{range})$
FO Aqr	0.88 (0.75, 35dof: 0.79–0.95)	poor fit
XY Ari	0.97 (0.83, 46dof: 0.80–1.13)	1.31 (1.13, 46dof: >1.25)
V405 Aur	0.99 (1.09, 47dof: 0.88–1.14)	1.32 (1.15, 49dof: >1.28)
BG CMi	1.15 (1.03, 44dof: 1.09–1.21)	1.25 (0.97, 46dof: 1.20–1.29)
V709 Cas	1.08 (1.22, 34dof: 0.91–1.13)	poor fit
TV Col	0.97 (1.06, 37dof: 0.92–0.99)	0.94 (1.02, 37dof: 0.88–0.97)
TX Col	0.74 (0.72, 37dof: 0.69–0.79)	0.72 (0.81, 37dof: 0.68–0.79)
EX Hya	0.44 (1.05, 37dof: 0.41–0.47)	0.47 (0.89, 37dof: 0.44–0.50)
AO Psc	0.60 (1.10, 35dof: 0.57–0.63)	0.61 (1.15, 35dof: 0.57–0.64)
V1223 Sgr	1.07 (0.65, 45dof: 0.98–1.15)	1.25 (0.95, 47dof: 1.21–1.27)
V1062 Tau	0.86 (0.72, 45dof: 0.80–1.04)	1.34 (0.75, 45dof: >1.28)
RX J1238–38	0.60 (1.00, 47dof: 0.57–0.66)	0.60 (1.01, 47dof: 0.57–0.66)
RX J1712–24	0.71 (0.87, 36dof: 0.68–0.78)	0.73 (0.54, 36dof: 0.63–0.77)

Table 3. The results for the fits to our intermediate polar data. The table follows the format of Table 2, with the exception of EX Hya and RX J1712–24 where the energy range was smaller (see text for details).

5.1 White Dwarf masses derived using X-ray data

We show in Table 4 the best fit masses for our sample derived using *RXTE* data along with the masses derived using *Ginga* data (taken from Cropper et al 1999) and *ASCA* data (taken from Ezuka & Ishida 1999). The masses derived using *Ginga* data were obtained using the same continuum model as used here while those derived using *ASCA* data were determined using the X-ray line analysis.

The mass estimates of Cropper et al (1999) using *Ginga* data were, on the whole, not very well constrained. Since *RXTE* has a higher energy response than *Ginga* our new mass estimates are much better constrained (the mean of the uncertainties in Tables 2 & 3 is $0.15 M_{\odot}$). It is therefore not surprising, that within the uncertainties, the *RXTE* and *Ginga* masses using our continuum method are consistent, with the exception of TX Col, which is heavier using the *RXTE* data.

Ezuka & Ishida (1999) determined the mass for 9 IPs using the emission line technique. However, most of those masses were not very well constrained. Only in the case of EX Hya (an uncertainty of $0.15 M_{\odot}$) and AO Psc ($0.23 M_{\odot}$) were the uncertainties comparable with that given here. In the case of EX Hya the masses derived from the continuum

and line methods are very similar (the best fit masses are within $0.03 M_{\odot}$) and in the case of AO Psc, the mass derived using the continuum method is marginally heavier than that of the line method. With a best fit mass of $0.45 M_{\odot}$, EX Hya is close to the minimum mass for isolated C-O core white dwarfs ($0.46 M_{\odot}$, Sweigart, Greggio & Renzini 1990). For masses lower than this, the white dwarf is expected to be a He-core white dwarf formed as a result of mass transfer in interacting binary stars.

Whilst we consider this sample of accreting magnetic white dwarfs masses to be the best constrained sample to have been derived using fits to X-ray data (using either the continuum or line method), a level of caution is appropriate. Our model of the post-shock region has undergone several improvements which make it more physically realistic. These changes have resulted in slightly different mass estimates. For instance, applying a gravitational potential across the height of the post-shock region resulted in lower masses ($\sim 0.1 M_{\odot}$) for masses above $1.0 M_{\odot}$. While we believe that the most important factors have been included in our model, other second order effects have not. For instance, it is assumed that the stream is approaching from infinity. In the case of IPs, which are thought to have a truncated

Source	<i>RXTE</i> M_{\odot}	<i>Ginga</i> M_{\odot}	<i>ASCA</i> M_{\odot}
V1432 Aql	0.98		
BY Cam	1.04	0.98	
V834 Cen	0.68	0.54	
AM Her	0.73	0.85	
BL Hyi	0.71		
V2301 Oph	0.75		
CP Tuc	0.68		
RX J2115–58	0.79		
FO Aqr	0.88	0.92	1.05
XY Ari	0.97	1.19	
V405 Aur	1.10		
V709 Cas	1.08		
TV Col	0.96	1.30	0.51
TX Col	0.73	0.48	0.66
BG CMi	1.20	1.09	
EX Hya	0.45	0.46	0.48
AO Psc	0.60	0.56	0.40
V1223 Sgr	1.10		1.28
V1062 Tau	0.90		
RX J1238–38	0.60		
RX J1712–24	0.71		0.68

Table 4. The best fit mass of mCVs determined using *RXTE* (this paper except RX J2115–58 which was taken from Ramsay et al 1999). The mass determined using *Ginga* data was taken from Cropper et al (1999) and the *ASCA* data from Ezuka & Ishida (1999).

accretion disk of some sort, this is clearly not the case. This will have a small effect on M_{wd} . As noted above, the model we use for the absorption is not appropriate and may have an effect on M_{wd} . In spite of this, we believe that the sample presented here is the best available with which to compare masses of magnetic white dwarfs found in accreting binary systems with that of non-magnetic white dwarfs.

5.2 The mass distribution of White Dwarfs mCVs

In our sample of polars we find a mean mass of $M_{wd}=0.80\pm 0.14 M_{\odot}$, while in our sample of IPs we find a mean mass of $M_{wd}=0.85\pm 0.21$. Taken as a whole, we find a mean mass for our mCVs of $M_{wd}=0.84\pm 0.20 M_{\odot}$. A better test is the Kolmogorov-Smirnov test (K-S test) which we can use to determine how likely it is that two distributions come from the same parent population. We find that using the K-S test there is a 81.4 per cent probability that our polar and IP samples do not come from the same parent population. We do not consider this to be significant.

To compare the combined distribution of our *RXTE* mCV sample we compare it with 5 samples of isolated non-magnetic white dwarf masses. Vennes et al (1997) determined masses for 90 white dwarfs which were detected in the *EUVE* all-sky survey (hereafter V97). Finley, Koester & Basri (1997) (FKB97) determined the masses for 174 white dwarfs which were taken from a sample of DA white dwarfs hotter than $\sim 25000\text{K}$. A total of 52 white dwarfs had mass determinations by Bragaglia, Renzini & Bergeron (1995) (BRB95) using a sample of bright field white dwarfs. Bergeron, Saffer & Liebert (1992) (BSL92) determined the

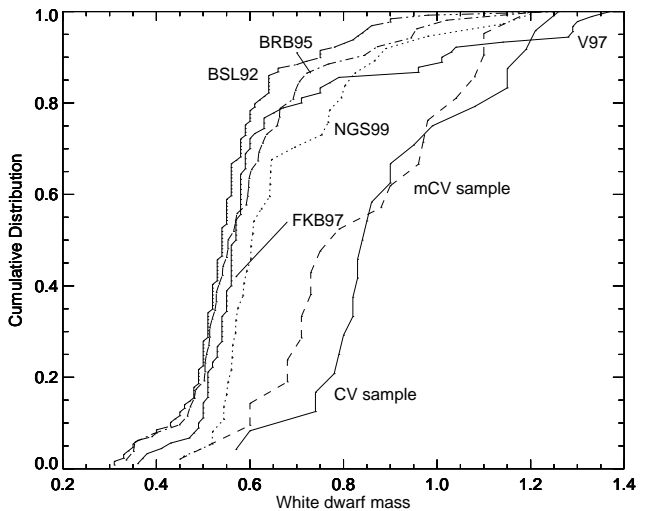


Figure 1. The cumulative distributions for the mass of magnetic white dwarfs in mCVs (this paper) and the mass of isolated non-magnetic white dwarfs: Napiwotzki, Green & Saffer (1999) (NGS99), Vennes et al (1997) (V97), Bergeron, Saffer, Liebert (1992) (BSL92), Bragaglia, Renzini & Bergeron (1995) (BRB95), Finley, Koester, Basri (1997) (FKB97). We also show the mass distribution of non-magnetic CVs taken from Ritter & Kolb (1998) (CV sample).

masses of 129 white dwarfs selected from the white dwarf catalogue of McCook & Sion (1987). Napiwotzki, Green & Saffer (1999) (NGS99) obtained masses for 43 white dwarfs selected from the *EUVE* and *ROSAT* WFC all-sky surveys. White dwarfs which were known to be in binary systems were excluded in our analysis. We show their cumulative distributions along with our mCV sample in Figure 1.

The most striking feature of Figure 1 is that while all the non-magnetic white dwarf distributions show a peak between $M_{wd}\sim 0.5-0.6 M_{\odot}$, our mCV sample is much more uniformly distributed. Performing a K-S test on the mCV distribution and the non-magnetic isolated white dwarf distributions we find that they are different with a greater than 99.99 percent probability. There is only a 9.3×10^{-12} probability that the mCV distribution and the distribution of BSL92 come from the same parent population.

We now compare the distribution of our *RXTE* mCV sample with that of non-magnetic CVs (nmCVs). For nmCVs the most reliable mass determinations are those where the system is a double-lined spectroscopic binary. There are 24 such systems in the catalogue of Ritter & Kolb (1998). We show the cumulative distribution of this sample in Figure 1. Similar to our mCV distribution, the nmCV distribution is also biased towards higher masses. The two distributions are different at the 89 per cent level: we do not consider this to be significant.

We now consider selection effects that can bias the mass distributions which we have considered. All samples of white dwarf masses are biased to some degree. For instance, FKB97 suggest that while studies based on EUV selected white dwarfs will not preferentially select high mass white dwarfs, white dwarfs with $M_{wd}<0.7 M_{\odot}$ that are over 400pc distant are strongly selected against since interstellar absorption will effectively obscure them. Indeed, there are significant differences between the various non-magnetic

white dwarf mass distributions. It is noteworthy that the EUV selected sample of V97 has a relatively high proportion of high mass systems: 12.2 percent of its sample have masses over $1.0M_{\odot}$ and 6.6 percent over $1.15M_{\odot}$. In the case of the nmCVs, a number of studies have looked at selection effects in detail (eg Ritter & Burkert 1986, Ritter et al 1991, Politano 1996). For a magnitude limited sample, the sample is biased towards more luminous objects which have a greater gravitational potential and are therefore more massive. These studies suggest that the apparent difference between the nmCV mass distribution and the isolated white dwarf mass distribution can largely be explained by this selection effect.

Selection effects are also important when considering our polar sample, many of which are discovered in soft X-rays. Similar to EUV selected white dwarfs, we may expect that low mass polars which are more distant than a few hundred pc, are selected against. On the other hand, we may expect that high mass polars are selected against for a different reason. This is because in order that high mass white dwarfs do not become unbound they must have a high internal magnetic pressure (Suh & Mathews 1999). Polars with high magnetic fields are not included in the *RXTE* database of polars because for high magnetic fields a greater proportion of the emission from the post shock region is emitted in the form of cyclotron radiation as opposed to bremsstrahlung radiation and are thus not strong hard X-ray emitters. Liebert (1988) found evidence for this in a sample of isolated white dwarfs. Other massive non-accreting magnetic white dwarfs have also recently been discovered: RX J0823.6–2525, $1.20 \pm 0.04 M_{\odot}$, 3MG (Ferrario, Vennes & Wickramasinghe 1998), RE J0317–858, $1.31\text{--}1.37 M_{\odot}$, $\sim 450\text{MG}$ (Ferrario et al 1997).

While many polars have been discovered in all-sky soft X-ray surveys such as that carried out using *ROSAT*, IPs are much stronger in hard X-rays. Apart from the *HEAO-1* all-sky hard X-ray survey which was undertaken in the late 1970's, no other such survey has been made. Those IPs discovered in hard X-rays are likely, therefore, to have been more luminous IPs and therefore more massive than average, leading to a possible bias in their mass distribution.

This study has found evidence that the distribution of white dwarf masses in mCVs is different from that of non-magnetic isolated white dwarfs in the sense that there is a bias towards heavier masses for white dwarfs in mCVs. On the other hand there is no significant difference between the distribution of white dwarf masses in mCVs and nmCVs. A detailed study of the various selection effects which are relevant to mCVs is beyond the scope of this paper, but such a study is needed to determine if (as in the case of nmCVs) selection effects can account for the apparent difference between the distribution of white dwarf masses in mCVs and isolated white dwarfs.

6 ACKNOWLEDGMENTS

I would like to thank the referee, Boris Gänsicke, and Mark Cropper for some useful comments on a previous draft of this paper.

REFERENCES

- Barwig, H., Ritter, H., Bärnbantner, O., 1994, *A&A*, 288, 204
 Bergeron, P., Saffer, R. A., Liebert, J., 1992, *ApJ*, 394, 228 (BSL92)
 Bragaglia, A., Renzini, A., Bergeron, P., 1995, *ApJ*, 443, 735 (BRB95)
 Cropper, M., Ramsay, G., Wu, K., 1998, *MNRAS*, 293, 222
 Cropper, M., Wu, K., Ramsay, G., 1999, In 'Annapolis Workshop on magnetic CVs', ASP Conf Ser, Vol 157, 325
 Cropper, M., Wu, K., Ramsay, G., Kocabiyyik, A., 1999, 306, 809
 Ezuka, H., Ishida, M., *ApJS*, 120, 277
 Ferrario, L., Vennes, S., Wickramasinghe, D. T., Bailey, J. A., Christian, D. J., 1997, *MNRAS*, 292, 205
 Ferrario, L., Vennes, S., Wickramasinghe, D. T., 1998, *MNRAS*, 299, L1
 Finley, D. S., Koester, D., Basri, G., 1997, *ApJ*, 488, 375 (FKB97)
 Fujimoto, R., Ishida, M., 1997, *ApJ*, 474, 774
 Liebert, J., 1988, *PASP*, 100, 1302
 McCook, G. P., Sion, E. M., 1987, *ApJS*, 65, 603
 Napiwotzki, R., Green, P. J., Saffer, R. A., 1999, *ApJ*, 517, 399 (NGS99)
 Politano, M., 1996, *ApJ*, 465, 338
 Ramsay, G., Cropper, M., Hellier, C., Wu, K., 1998, *MNRAS*, 297, 1269
 Ramsay, G., Potter, S., Cropper, M., Buckley, D., Harrop-Allin, M. K., submitted, *MNRAS*
 Ritter, H., Burkert, A., 1986, *A&A*, 158, 161
 Ritter, H., Politano, M., Livio, M., Webbink, R. F., 1991, *ApJ*, 376, 177
 Ritter, H., Kolb, U., 1998, *A&AS*, 129, 83
 Silber, A. D., Remillard, R. A., Horne, K., Bradt, H. V., 1994, *ApJ*, 424, 955
 Sweigart, A. V., Greggio, L., Renzini, A., 1990, *ApJ*, 364, 527
 Suh, I.-S., Mathews, G. J., submitted *ApJ*, astro-ph/9906239
 Wu, K., Chanmugam, G., Shaviv, G., 1994, *ApJ*, 426, 664
 Vennes, S., Thejll, P. A., Galvan, R. G., Dupuis, J., 1997, *ApJ*, 480, 714 (V97)